5
Pulsed magnetron heating experiments on transient toroidal helium plasmas

We experimentally studied the evolution of a transient toroidal helium plasma, subjected to a high power 2.46 GHz microwave pulse. We discuss in detail the design of the pulsed magnetron source and determine its electrical characteristics during these experiments. To apply the 1.75 kW high power microwave pulse to the toroidal plasma, we designed a 2.465 GHz iris coupled rectangular microwave cavity. We discuss the effect of the microwave pulse on the toroidal plasma, and elaborate on the dark space that is observable between the microwave generated plasma and the toroidal plasma. We determine that the 100 µs long microwave pulse attains a sub-microsecond rise time and discuss the frequency droop during this pulse. Finally, we present a poloidal excitation temperature profile of the toroidal plasma by applying a standard Boltzmann analysis to two tomographic reconstructions of the toroidal plasma, obtained from images recorded at two different wavelengths.

5.1 Introduction

The endeavours presented in this work all have been carried out while keeping in mind the desire to realise self-organising knotted magnetic structures in plasma. So far, our main concern has been the study of transient toroidal helium plasmas, however, their limited lifetime, which is considerably less than 100 µs, unfortunately hinders the realisation of these structures.

In this chapter we present our first experiments aimed at extending the lifetime of these toroidal plasmas, through heating of these structures using microwave radiation, and discuss the observations and preliminary steps made in this direction. The main difficulty with this venture is once more, the limited lifetime of these plasmas, which

necessitates a pulsed nature of these experiments if a detailed study of its effects is desired.

In what follows we present the design of the pulsed magnetron source used in our experiments on transient toroidal helium plasmas, and characterise its behaviour during these experiments. We discuss the integration of a 2.465 GHz microwave cavity into our existing set-up used to study the toroidal plasmas, and present optical recordings of the evolution of a toroidal plasma subjected to a high power 2.46 GHz microwave pulse. We discuss the observed effects, and elaborate on the additional plasma structure generated by the microwave field near the toroidal plasma.

Finally, we will present a poloidal excitation temperature profile of the toroidal plasma, including the surrounding microwave generated plasma structure, obtained from recordings captured 50 µs after the creation of the laser-induced breakdown plasma responsible for the generation of the toroidal plasma.

5.2 *Design of the pulsed magnetron source*

The microwave generators that are generally used, for example, for atomic emission spectroscopy and plasma ion sources, are continuous microwave generators. However, because we are investigating transient toroidal helium plasmas with a lifetime which is considerably less than 100 µs, we need a pulsed microwave source that matches this time-scale, in order to investigate the effects of heating at different moments during the evolution of our toroidal plasma. Additionally, due to the limited time available to add energy to the toroidal plasma, a high power source is mandatory. For this reason we have opted for a magnetron as the source of microwave radiation.

Trivially, the microwave pulses generated must have at least a short rise time, to be able to create short pulses. The physical processes at work in a magnetron unfortunately conflict with this requirement, because for a magnetron it takes time to start oscillating as a result of the stochastic nature of this process. The rising edge of the high-voltage pulse must therefore spend a finite time in the so-called Hartree region to ensure that the oscillations start properly in each pulse. Furthermore, because the magnetron typically operates at about 4 kV, driving the capacitance of the wiring, the transformers and the magnetron itself, poses limitations on the rise time of the pulse.

Our adopted solution is to continuously operate the magnetron on an extremely low power, such that the magnetron has the ability

to start oscillating properly. Subsequently, while the magnetron is oscillating at low power, we generate a high power pulse by very rapidly increasing the current through the magnetron. This significant increase in current is accompanied by just a small increase in the magnetron voltage due to the low dynamical resistance of the magnetron above the Hartree voltage. In radar applications, where high spatial resolution and minimum range coverage to within a few metres are required, for example, for active seekers for missiles, a magnetron is operated using a pedestal modulation technique,[1] improving upon our adopted scheme.

[1] Nyswander et al. 1976.

The high-voltage magnetron pulser

In figure 5.1 we present a simplified schematic of the high-speed high-voltage pulser used to drive the magnetron in the experiments presented in this chapter. Auxiliary components such as those used for voltage and current measurements have been omitted for reasons of readability. The high-voltage transformers and passive components, as well as the magnetron itself, are components that can be readily found in domestic microwave ovens. In this experiment a Samsung OM75P magnetron has been used. The filament transformer is a tailor-made low capacitance transformer. Standard variable auto-transformers have been used to vary the primary voltage of the high-voltage and filament transformers.

The pulser is designed around two Greinacher voltage doublers which double the secondary voltage of the two mains[2] connected high-voltage transformers. Depending on the settings of the auto-transformers, voltages of up to 5.5 kV can be generated. To be able to generate microwave pulses with sub-microsecond rise times, the

[2] The mains is also referred to as utility power.

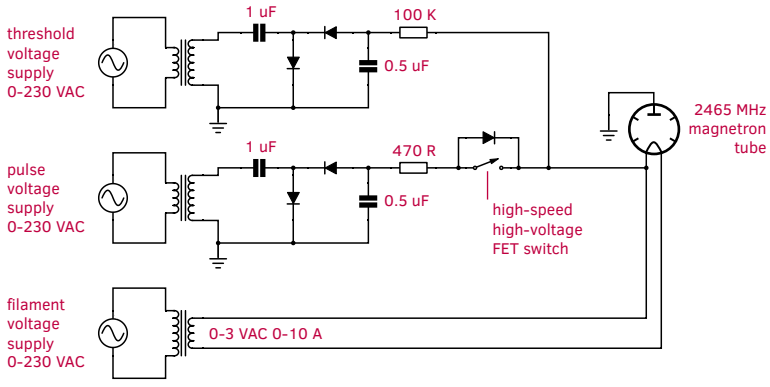

Figure 5.1: Simplified schematic of the high-speed high-voltage pulser used to drive the magnetron in the presented heating experiments on transient toroidal helium plasmas. Auxiliary components such as those used for voltage and current measurements have been omitted for reasons of readability.

magnetron voltage is biased using a 100 K resistor, which brings the magnetron voltage to a threshold voltage of approximately 4 kV.

A 470 R series resistor is used to create a rudimentary current source for driving the low dynamical resistance of the magnetron, and is switched using a high-speed high-voltage FET switch (Behlke HTS 81-12-B) whose trigger signal is generated by the same trigger system used for the generation and analysis of the toroidal plasmas. This system is build around a digital delay generator (Stanford Research Systems DG645) and an in-house designed FPGA (field-programmable gate array) based reconfigurable pulse generator. The particulars of the trigger system are explained in more detail in section 2.2.

Integration of a microwave cavity into the plasma reactor

The high power microwave pulses, generated by the high-voltage magnetron pulser, have to be applied to our toroidal plasma. In plasma research different approaches exist for the coupling of microwave radiation to a plasma.

We initially started with a directly coupled monolithic rectangular microwave cavity,[3] where the magnetron antenna is mounted directly into the resonant cavity. Although the approach is very appealing, primarily because of its simplicity, we ran into issues where the magnetron did not start to oscillate properly, or oscillated at an incorrect frequency, or with low power.

[3] Spanel et al. 2004.

We attributed this to the fact that the magnetron starts to oscillate at a frequency different from the resonance frequency of the cavity. As a result, the power reflected off the cavity is injected into the magnetron, thereby influencing its start-up behaviour.

Different improved approaches exist, where the resonant cavity is separated from the magnetron.[4] These, we found, are bothered by similar start-up difficulties. In the end we opted for a more conventional set-up, whereby the magnetron is completely isolated from the rest of the microwave set-up using a microwave isolator, thereby preventing the injection of reflected power into the magnetron.

[4] Broekaert et al. 2004; Matusiewicz 1992; Hammer 2008.

In figure 5.2 we present a simplified schematic[5] of the combined pulsed magnetron set-up and the pulsed high power optical set-up, used for the experiments presented in this chapter.

[5] For a more lively impression of the experimental set-up we refer to photo 3 on page 105.

The pulsed magnetron set-up consists of a 2.465 GHz iris coupled TE101 mode $\lambda_g/2$ rectangular microwave cavity, a tailor-made three stub tuner and a coaxial to wave-guide transition. The rectangular wave-guide stub tuner and the microwave cavity are mounted directly into

the plasma reactor. This is not the most ideal approach, because it necessitates the use of a vacuum sealed coaxial to wave-guide transition and a vacuum sealed wave-guide entrance into the plasma reactor. But just as with our 57 GHz diagnostic experiments presented in chapter 4, it proved to be the most practical means to integrate these experiments into our existing set-up.

The microwave cavity is positioned in such a way that the anti-node of the electric field of the TE101 mode coincides with the focal point of the lens generating the laser-induced breakdown plasmas from which the toroidal plasmas emerge.

The microwave cavity is further equipped with beyond cut-off view ports (not shown) such that the laser pulses can safely enter and exit the cavity. In a similar fashion, side view images of the toroidal plasma can

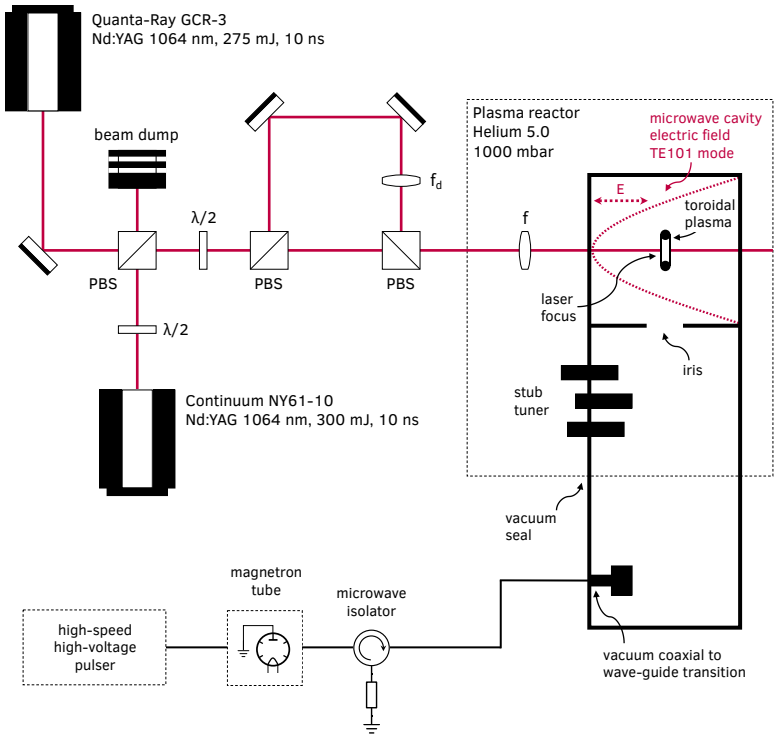

Figure 5.2: Simplified schematic of the combined pulsed magnetron set-up and the pulsed high power optical set-up used for the presented experiments. The pulsed magnetron set-up consists of a 2.465 GHz iris coupled TE101 mode $\lambda_g/2$ rectangular microwave cavity, a tailor-made three stub tuner and a coaxial to wave-guide transition. The rectangular wave-guide stub tuner and the microwave cavity are mounted directly into the plasma reactor. The microwave cavity is positioned in such a way that the anti-node of the electric field of the TE101 mode coincides with the focal point of the lens generating the laser-induced breakdown plasmas. The high power optical set-up is identical to the set-up used to investigate the transient toroidal helium plasmas as presented in chapter 2. For a more lively impression of the experimental set-up we refer to photo 3 on page 105.

be obtained, just like in the experiments presented in chapter 2.

The guide wavelength for our aluminium rectangular wave-guide, having internal dimensions of 90 x 40 mm, is approximately 165 mm. The $\lambda_g/2$ microwave cavity is coupled to the feeding wave-guide using an iris with an aperture diameter of 21 mm. The described vacuum seals in the plasma reactor wall, and in the coaxial to wave-guide transition, ensure that the experiments can be performed in a pure helium atmosphere.

High power 2.46 GHz microwave pulses of up to 1.75 kW have been generated using the high-voltage magnetron pulser described in the previous subsection. The microwave isolator protects the operation of the magnetron against power reflected off a possibly detuned microwave cavity, as a result of the presence of plasma in the cavity. The high power optical set-up is identical to the set-up used to investigate the transient toroidal helium plasmas, and for a detailed description thereof we refer to section 2.2.

5.3 *Pulsed magnetron heating experiments on transient toroidal helium plasmas*

Using the pulsed magnetron source presented in the previous section, we performed experiments on the transient toroidal helium plasmas studied extensively in chapter 2. In this section, we present an analysis of the optical recordings captured during these experiments, and characterise the behaviour of the magnetron pulser.

Optical analysis of the pulsed magnetron heating experiments

The transient toroidal helium plasmas studied in this section have been generated by a single laser-induced breakdown plasma, created in quiescent atmospheric pressure helium gas at room temperature. The laser pulse energy used to create the breakdown plasmas was 250 mJ.

For our optical analysis we recorded side view images through a view port in the microwave cavity as described in the previous section. All images have been captured using a fixed gate width of 250 ns and a fixed gain of 255. Because of the small fluctuations visible in the recordings, all images have been averaged over 50 repetitions, to increase the signal to noise ratio. Furthermore, all images have been corrected for flat field and background emission, and to aid in a quantitative analysis, all images have been captured through a 10 nm bandpass filter with a centre wavelength of 590 nm. For further experimental details, and a

motivation of the above, we refer to sections 2.2–2.3.

In figure 5.3 we present selected side view images of the evolution of a transient toroidal helium plasma, starting from 20 µs after the creation of a laser-induced breakdown plasma. The top row shows the familiar evolution in the absence of microwave radiation. The bottom row shows the same time span, whereby during the whole presented evolution the magnetron has been operational and microwave radiation was present in the cavity in which the toroidal plasma was generated. In figure 5.4 the spectral radiant intensity of the observed evolution is presented.

The microwave pulse in this experiment extends from 20 µs to 120 µs. The beginning of the microwave pulse does not leave any observable effect, neither in the optical images nor in the spectral radiant intensity. However, the end of the pulse is clearly visible in the sharp decline of the spectral radiant intensity at 120 µs.

In the optical recordings of figure 5.3, the toroidal plasma seems to be unaffected by the microwave field. However, from 52 µs onward, we observe that the microwave field generates additional plasma, and surprisingly, this microwave plasma is generated at a distance from the region where the toroidal plasma has been observed, even after the toroidal plasma itself already is extinguished. After 76 µs we see that this region is also filled with plasma generated by the microwave field.

The observed distance between the microwave generated plasma and the toroidal plasma is reminiscent of the dark spaces found in a glow discharge.[6] In the Aston dark space of a glow discharge, the electrons

[6] Fridman 2008, p. 175.

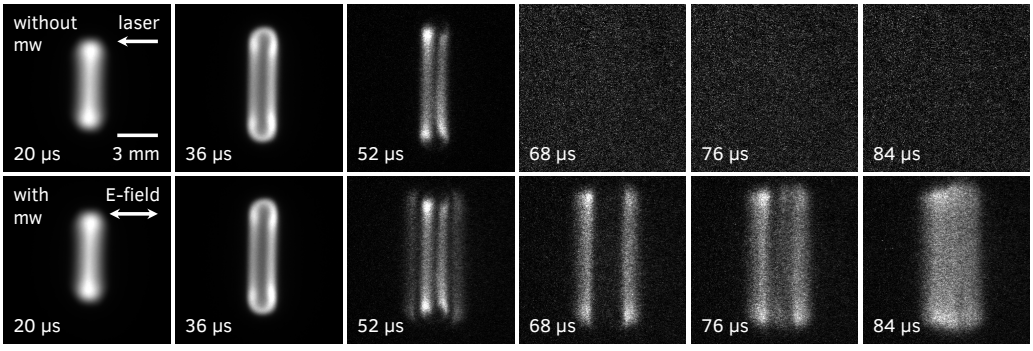

Figure 5.3: Selected side view images of the evolution of a transient toroidal helium plasma, starting from 20 µs after the creation of a laser-induced breakdown plasma. The top row shows the familiar evolution in the absence of microwave radiation, whereas the bottom row shows the same time span, whereby during the whole presented evolution the magnetron has been operational and microwave radiation was present in the cavity. All images have been averaged over 50 exposures and captured through a 10 nm bandpass filter with a centre wavelength of 590 nm. All images have been individually normalised to their maximum intensity to respect the large dynamic range in intensity of the entire evolution. Laser pulse energy: 250 mJ, focal length focussing lens: 50 mm, helium gas pressure: 1003 mbar, ICCD camera gate width: 250 ns, ICCD camera gain: 255.

ejected from the cathode, through secondary electron emission, do not have sufficient energy for the excitation of atoms, and therefore a dark space forms. The electrons are subsequently accelerated in the electric field of the glow discharge, and when they have gained sufficient energy to excite atoms, the dark space ends.

The dark space observed around the toroidal plasma can be explained when we assume that the electrons needed for the generation of the microwave plasma surrounding the toroidal plasma, are ejected from the toroidal plasma itself, but just like in the Aston dark space of a glow discharge, do not yet have sufficient energy for the excitation of helium atoms. Because of the quasi neutrality of the toroidal plasma, not all of its electrons can participate in this process, only the high energy electrons that manage to overcome the electrical potential of the ion charge density, can escape from the surface of the toroidal plasma. These electrons are then accelerated in the electric field of the microwave pulse, until they have gained sufficient energy for the excitation of the helium atoms surrounding the toroidal plasma.

A similar dark space has been observed in experiments where we subjected the toroidal plasma to a high-voltage pulse. In figure 5.5 we present the evolution of such a measurement, where the toroidal

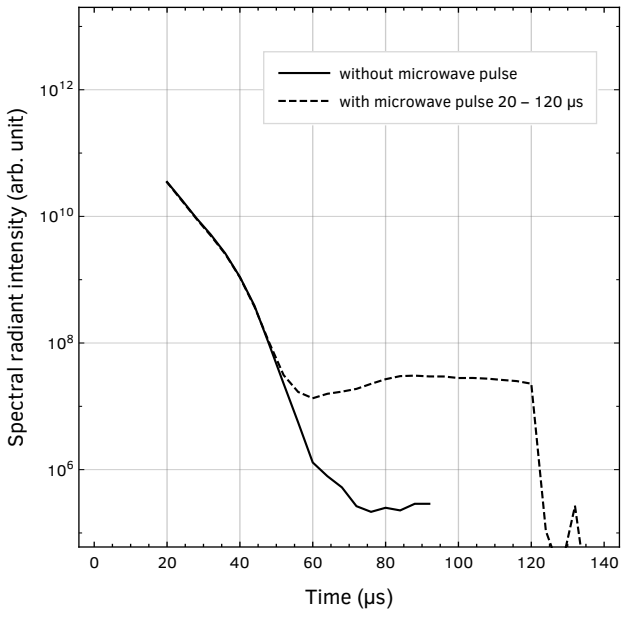

Figure 5.4: Spectral radiant intensity of the evolution presented in figure 5.3. Measurements have been recorded at a 4 µs interval but for clarity only selected images have been presented in figure 5.3.

plasma has been subjected to a +4 kV high-voltage pulse, showing with nanosecond temporal resolution, the emission of an ionisation wave propagating away from the toroidal plasma. Prior, an ionisation channel can be seen to form, from the high-voltage tip to the toroidal plasma. Between the toroidal plasma and the ionisation wave, and similarly between the ionisation channel and the toroidal plasma, a dark space can clearly be observed.

These dark spaces can be explained on similar grounds as the dark space around the toroidal plasma in the presence of a microwave field. Because the high-voltage tip is positively charged, the toroidal plasma acts as a cathode, resulting in an Aston dark space between the ionisation channel and the toroidal plasma. Similarly, the dark space between the ionisation wave and the toroidal plasma can be regarded as the anode dark space of a glow discharge, where electrons are removed from the vicinity of the toroidal plasma as a result of its positive potential with respect to the plasma reactor.

The fact that the toroidal plasma seems to be unaffected by the microwave field could be anticipated for if we take into consideration the evolution of the electron number density obtained in chapter 4. The critical electron number density for 2.46 GHz radiation is more than a factor of 500 lower than for the 57 GHz radiation used in those experiments. An examination of the results presented in figure 4.9 reveals that the electron number density attains the same order of magnitude as the critical electron number density for 2.46 GHz radiation at around 75 µs. Before that time, the 2.46 GHz microwave field cannot be expected to penetrate the toroidal plasma, as is in clear agreement with the observations presented in figure 5.3.

We have to note that the results presented in chapter 4 have been obtained after a number of coarse approximations. Nevertheless, the consensus of the observations presented here and the electron number density obtained in chapter 4 seems trustworthy.

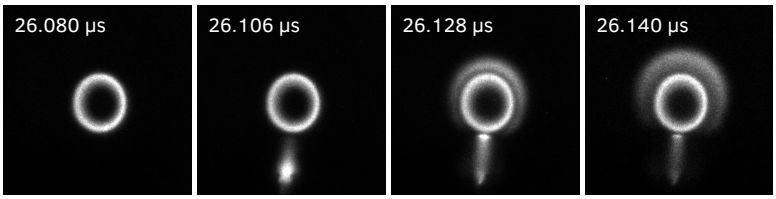

Figure 5.5: Evolution of a representative measurement where the toroidal plasma has been subjected to a +4 kV high-voltage pulse, showing with nanosecond temporal resolution, the emission of an ionisation wave propagating away from the toroidal plasma. Prior, an ionisation channel can be seen to form, from the high-voltage tip (at the bottom of the image, but not visible) to the toroidal plasma.

Characterisation of the pulsed magnetron source

In the remainder of this section we present the electrical characteristics of the pulsed magnetron source, determined during the experiments presented in the previous subsection.

As explained in section 5.2 on the design of the pulsed magnetron source, before the actual generation of high power microwave pulses, the magnetron is brought into the Hartree region, to ensure that the magnetron starts to oscillate properly, but does so with minimal power. In the described experiments this has been realised by increasing the pulser threshold voltage to 4.1 kV. At this voltage the current through the magnetron was measured to be 8.1 mA.

Obviously, before a magnetron can oscillate, as it is just a kind of vacuum tube, the magnetron filament has to be heated in order to ensure that thermal electron emission can occur. In our experiments we used a filament voltage of 2.6 VAC resulting in a filament current of 7.1 A. We found that by slightly adjusting the filament current during an experiment, the oscillation frequency of the magnetron could be tuned to an optimal frequency for our microwave cavity.

The pulse voltage used to generate the high power pulses was set to

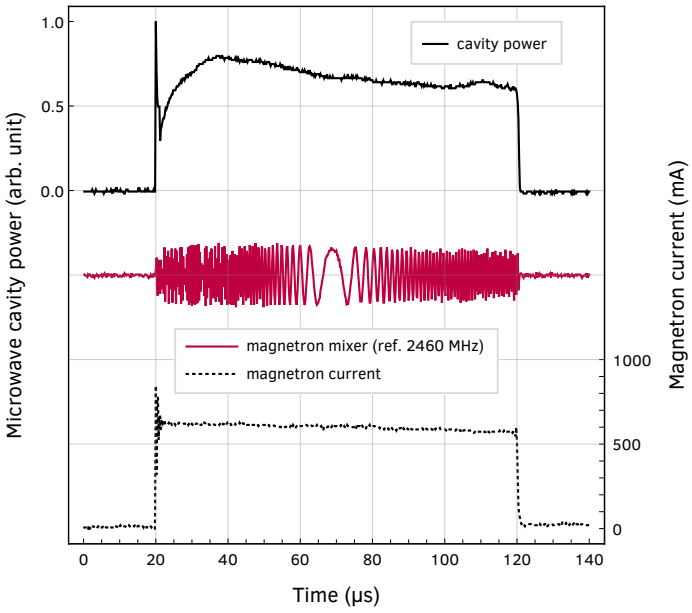

Figure 5.6: Evolution of the microwave cavity power and the magnetron current for the experiment whose optical evolution is presented in figure 5.3, together with a magnetron mixer signal, obtained by mixing stray radiation emitted by the magnetron and received by a simple loop antenna, with a fixed reference frequency of 2460 MHz.

5.2 kV. Note that this voltage is measured before the 470 R series resistor, so that the actual magnetron voltage is considerably lower due to its low dynamical resistance above the Hartree voltage.

In figure 5.6 we present, for the experiment described in the previous subsection, the evolution of the microwave cavity power and the magnetron current, together with a magnetron mixer signal, obtained by mixing stray radiation emitted by the magnetron and received by a simple loop antenna, with a fixed reference frequency of 2460 MHz.

From the magnetron mixer signal, we derived the evolution of the magnetron frequency during the experiment, by analysing its zero-crossings. The evolution thus obtained is presented in figure 5.7.

The slight decline in the magnetron frequency can be understood from the observed decline in current through the magnetron. In order to mitigate this change in frequency, the generation of the toroidal plasmas has been synchronised with the mains, such that both capacitors of the Greinacher voltage doubler will be used as an energy source for the magnetron pulse, thereby limiting the current droop through the magnetron. Operating the pulsed magnetron source synchronised with the mains thereby reduces the experimental fluctuations that would be caused by the generation of the magnetron pulse at arbitrary times

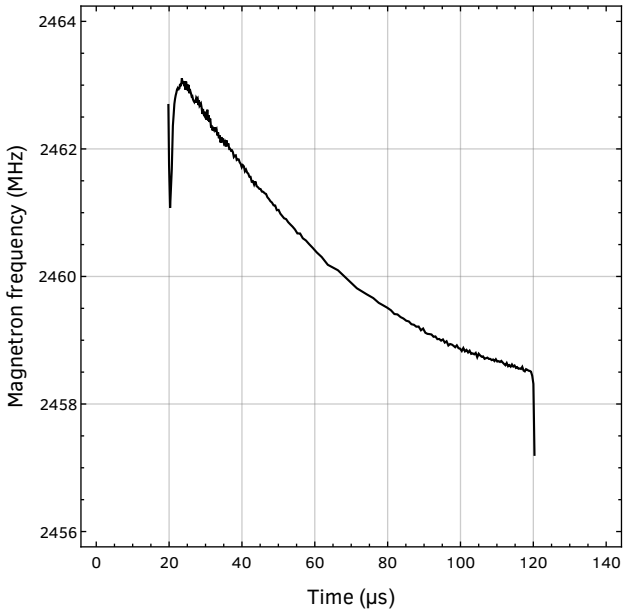

Figure 5.7: Evolution of the magnetron frequency during the generated high power microwave pulse, obtained by analysing the zero-crossings of the magnetron mixer signal presented in figure 5.6.

during a mains voltage cycle. A possible improvement of the stability of the magnetron frequency can be obtained by injection-locking the magnetron to an external low-power frequency reference.[7]

[7] Tahir et al. 2006.

From the recordings presented in figure 5.6 we can see that the average current through the magnetron is approximately 600 mA. Combined with a magnetron voltage of about 4.1 kV we find that the electrical power delivered to the magnetron is approximately 2.5 kW. The efficiency of the magnetron has been measured[8] to be approximately 70% which implies a microwave pulse power of 1.75 kW. Unfortunately, we did not have the ability yet to measure the absolute power inside the microwave cavity, so we could not quantitatively obtain a value for the microwave cavity power.

[8] The efficiency of the magnetron has been determined in an isolated set-up, disconnected from the microwave cavity, where the power of the pulse has been measured using a 50 dB attenuator.

The recorded evolution of both the magnetron current and the microwave cavity power, indicates that the rise and fall times of the microwave pulses are very fast, and that sub-microsecond rise times are attained.[9] The cavity power shows complicated behaviour that needs further analysis, but it is tenable to conclude that the cavity power is affected by the varying magnetron frequency, through the frequency response of the cavity, as well as by the presence of plasma in the cavity.

[9] During the determination of the magnetron efficiency mentioned above, we generated microwave pulses with a length of 10 µs and observed rise and fall times of less than 500 ns.

The observed detuning of the cavity resonance frequency of about 5 MHz is caused by the presence of plasma in the cavity. Inserting a small amount of dielectric material into a resonant cavity is known to cause the resonance frequency to shift slightly.[10] For our toroidal plasma this can be understood when considering the toroidal plasma to be a conductor situated in parallel to the cavity walls, perpendicular to the direction of the electric field, thereby acting as a capacitor which lowers the resonance frequency of the microwave cavity.

[10] Waldron 1960.

5.4 *Poloidal excitation temperature profile of transient toroidal helium plasmas*

The observation that the microwave generated plasma surrounding the toroidal plasma, and the toroidal plasma itself, are essentially two distinct plasmas, raises the question of how these plasmas differ in their optical properties and how they are spatially distributed.

In a first attempt to answer these questions, we recorded images during the aforementioned experiments using two different 10 nm bandpass filters that enclose the atomic helium emission lines at 587.6 nm and 706.5 nm, motivated by the same reasoning set out in section 2.3. In addition to a filter with a centre wavelength of 590 nm

(Thorlabs FB590-10) used for most images presented in this work, additional images have been recorded through a filter with a centre wavelength of 710 nm (Thorlabs FB710-10).

To be able to spatially discern from where the emission of both plasmas originate, and even more importantly, because we set out to determine an estimate of the excitation temperature of both plasmas, it is instrumental to tomographically reconstruct the poloidal radiant intensity profile of both plasmas using the method described in section 2.5. Because the excitation temperature will be determined using a standard Boltzmann analysis,[11] which utilises relative intensities, or ratios, of the atomic helium emission lines, it is evident that a tomographic reconstruction is necessary.

[11] Griem 1997, p. 279; Monfared et al. 2011; Gulec et al. 2015.

In figure 5.8 we present side view images of the microwave generated plasma surrounding the toroidal plasma, and the toroidal plasma itself, recorded through two different bandpass filters as explained above, together with their poloidal radiant intensity profile obtained through a tomographic reconstruction. The poloidal radiant intensity profiles are presented in black and white, as well as in contrast enhanced false colour, to better visualise the core of the toroidal plasma.

The side view images have been captured 50 µs after the creation of the laser-induced breakdown plasma responsible for the generation of the toroidal plasma. To further increase the signal to noise ratio, the gate width has been increased to 1 µs and all recordings have been averaged

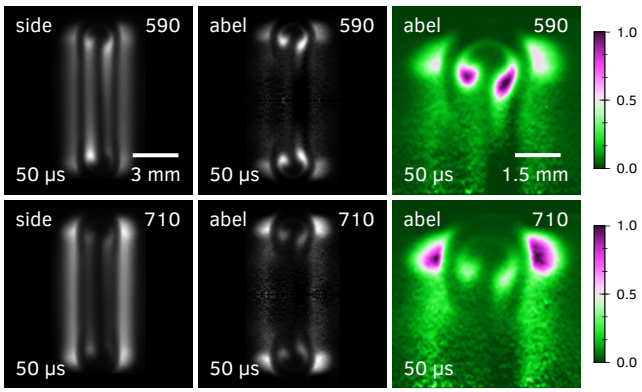

Figure 5.8: Side view images of the microwave generated plasma surrounding the toroidal plasma, and the toroidal plasma itself, recorded through two different 10 nm bandpass filters with a centre wavelength of 590 nm resp. 710 nm, together with their poloidal radiant intensity profile obtained through a tomographic reconstruction. The side view images (left) have been captured 50 µs after the creation of the laser-induced breakdown plasma responsible for the generation of the toroidal plasma. The poloidal radiant intensity profiles are presented in black and white (centre) as well as in contrast enhanced false colour (right) to better visualise the core of the toroidal plasma. Note that the images have been individually normalised to their maximum intensity to respect their large dynamic range, and that the contrast enhanced false colours do not share the same absolute scale between the 590 nm and 710 nm recordings.

over 1000 repetitions. The experimental conditions are otherwise similar to those presented in section 5.3.

It is clear that the side view images exhibit a slight asymmetry between their top and bottom halves, which influences the tomographic reconstruction as explained in section 2.4. An assessment of the obtained poloidal radiant intensity profiles nevertheless indicates that this effect seems to be limited for these reconstructions.

From the presented images it is evident that the toroidal plasma is the brightest in the images recorded at 590 nm, whereas this is the converse for the images recorded at 710 nm. This is an indication that the excitation temperature of the microwave generated plasma surrounding the toroidal plasma, and the toroidal plasma itself, are different.

Using the tomographically reconstructed images from the recordings captured through the 590 nm and 710 nm bandpass filters, we can obtain, by applying a standard Boltzmann analysis to each and every pair of pixels, a poloidal excitation temperature profile of our toroidal plasma at 50 µs. The result of this analysis is shown in figure 5.9, where we present a contour plot of the poloidal excitation temperature profile, and an image showing the same temperature contours combined with the poloidal radiant intensity profile of the 590 nm recording presented in figure 5.8.

The combined temperature contour plot in figure 5.9 shows that the core of the toroidal plasma reaches excitation temperatures in excess of 4500 K. These high temperature regions coincide with the high intensity regions visible in the poloidal radiant intensity profile. A small misalignment can be observed, which we attribute to a possible image

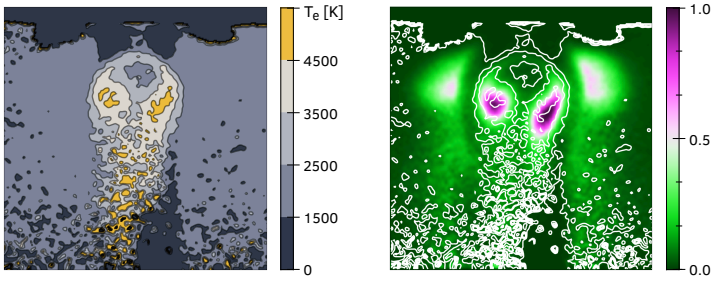

Figure 5.9: (left) Contour plot of the poloidal excitation temperature profile of the microwave generated plasma surrounding the toroidal plasma, and the toroidal plasma itself, obtained from recordings captured 50 µs after the creation of the laser-induced breakdown plasma responsible for the generation of the toroidal plasma. (right) An image showing the same temperature contours combined with the poloidal radiant intensity profile of the 590 nm recording presented in figure 5.8. The structure visible above the toroidal plasma, across the width of the image, is an artefact of the tomographic reconstruction. The poloidal excitation temperature profile has been obtained by applying a standard Boltzmann analysis to each and every pair of pixels of the poloidal radiant intensity profiles presented in figure 5.8.

displacement between the 590 nm and 710 nm recordings as a result of slightly tilted optical filters, but this requires further investigation.

The microwave generated plasma surrounding the toroidal plasma seems to attain a uniform excitation temperature of the order of 2000 K. In the temperature contour plot the microwave generated plasma is not discernible, instead the entire region outside the toroidal plasma seems to have a uniform temperature. This can be understood when we realise that the optical components used to image the toroidal plasma scatter slightly, and that this scattered light, however minimal, ends up in regions where there is no plasma emission at all. Applying the Boltzmann analysis to these regions, however weak they are, will result in the temperature of the closest source of plasma emission.

Although the excitation temperatures found seem reasonable,[12] a better approach would be to determine the temperature through a Boltzmann analysis based on multiple intensity ratios, obtained from additional atomic helium emission lines.

[12] Gulec et al. 2015; Monfared et al. 2011; Quintero et al. 1997.

As a first step towards this approach, we determined the excitation temperature through an additional measurement using a 10 nm bandpass filter with a centre wavelength of 670 nm (Thorlabs FL670-10) enclosing the atomic helium emission line at 667.8 nm. Unfortunately, we found that the obtained temperature was highly sensitive to our spectral amplitude calibration. Although only line intensity ratios are a relevant measure, the bandpass filters still need to be calibrated against a known amplitude calibrated spectrum.[13] In this process we found that the optical components used in our imaging set-up significantly filter the light captured from our plasma, further complicating this calibration.

[13] Specifically, the optical transmission of the bandpass filters needs to be determined precisely at the wavelength of the atomic helium emission lines.

Finally, we note that the above analysis provides very reasonable results, compared to the findings in related works, but for detailed and high temperature resolution imaging we need to further substantiate the applicability of the Boltzmann analysis,[14] for example, whether it is permissible to assume local thermodynamic equilibrium and whether the presence of metastable helium affects the analysis.

[14] Quintero et al. 1997; Ohno et al. 2006; Boivin et al. 2001; Griem 1997, p. 279.

5.5 *Conclusion and discussion*

In this chapter we have presented optical recordings of the evolution of a transient toroidal helium plasma subjected to a high power 2.46 GHz microwave pulse, and discussed the electrical characteristics of the pulsed magnetron source during these experiments. We discussed, in detail, the design of the pulsed magnetron source as well as the integration of a 2.465 GHz iris coupled rectangular microwave cavity

into our existing set-up for the generation and analysis of toroidal helium plasmas. The microwave cavity has been designed to apply the high power microwave pulses to the toroidal plasma and is mounted directly into the plasma reactor.

The toroidal plasmas studied have been generated by a single laser-induced breakdown plasma, created in quiescent atmospheric pressure helium gas at room temperature. The laser pulse energy used to create the breakdown plasmas was 250 mJ.

We found that the toroidal plasma is unaffected by the microwave pulse, and attributed this to the observation, based on the earlier performed diagnostics experiments at 57 GHz, that the electron number density is far above the critical electron number density for 2.46 GHz radiation. From approximately 52 µs onward, we observed that the microwave pulse generated additional plasma at a distance to the toroidal plasma.

We discussed the dark space between the toroidal plasma and the microwave generated plasma, and presented an experiment whereby the toroidal plasma has been subjected to a +4 kV high-voltage pulse, and where a similar dark space has been observed between the generated ionisation wave and the toroidal plasma.

The evolution of the microwave cavity power and the magnetron current indicate that sub-microsecond rise times are attained and that 2.46 GHz microwave pulses of up to 1.75 kW can be generated. During the 100 µs long microwave pulse, a frequency droop of 5 MHz is observable. We proposed a possible improvement of the stability of the magnetron frequency by injection-locking the magnetron to a low power reference frequency.

We presented a poloidal excitation temperature profile of the microwave generated plasma surrounding the toroidal plasma, and the toroidal plasma itself, obtained from recordings captured through two different 10 nm bandpass filters, captured 50 µs after the creation of the laser-induced breakdown plasma responsible for the generation of the toroidal plasma.

Because the excitation temperature has been determined through a standard Boltzmann analysis, the recorded images have been tomographically reconstructed, to ensure that the intensity ratios of the atomic helium emission lines are a meaningful quantity. We found that the microwave generated plasma and the toroidal plasma are two distinct plasmas. The core of the toroidal plasma has been determined to reach temperatures in excess of 4500 K, whereas the microwave generated plasma appears to have a uniform temperature of

about 2000 K. We discussed the applicability of the Boltzmann analysis, motivated by the sensitivity of the excitation temperature on the spectral amplitude calibration of the imaging set-up.

The results presented above indicate that microwave heating of a region near the toroidal plasma with the developed pulsed magnetron source is feasible. However, reheating of the actual toroidal plasma does not occur. Currently, new microwave cavity designs are being developed, in order to investigate reheating through induction. The use of a cylindrical microwave cavity mode is of particular interest here and experiments are currently underway to implement this mode, in order to sustain the toroidal plasma and realise the sought after magnetic field configurations.

These kinds of sustainable plasma configurations, combined with toroidal fluid flow, are currently also considered in collaboration with the Dutch Institute for Fundamental Energy Research (DIFFER), in order to realise a chemical reactor in which the burning of fuel is replaced by a microwave heated plasma powered by renewable energy, therewith connecting to the quest to reduce CO_2 emission.